Title

Anticystogenic activity of a small molecule PAK4 inhibitor may be a novel treatment for autosomal dominant polycystic kidney disease

Journal

Kidney International, 92(4)

ISSN

0085-2538

Authors

Hwang, Vicki J
Zhou, Xia
Chen, Xiaonan
et al.

Publication Date

2017-10-01

DOI

10.1016/j.kint.2017.03.031

Peer reviewed

HHS Public Access

Author manuscript

Kidney Int. Author manuscript; available in PMC 2018 October 01.

Published in final edited form as:

Kidney Int. 2017 October ; 92(4): 922–933. doi:10.1016/j.kint.2017.03.031.

Anti-cystogenic activity of a small molecule PAK4 inhibitor may be a novel treatment for Autosomal Dominant Polycystic Kidney Disease

Vicki J. Hwang[1], **Xia Zhou**[4], **Xiaonan Chen**[1,3], **Josephine Trott**[1], **Omran Abu Aboud**[1], **Kyuhwan Shim**[5], **Lai Kuan Dionne**[5], **Kenneth J. Chmiel**[1], **William Senapedis**[6], **Erkan Baloglu**[6], **Moe R. Mahjoub**[5], **Xiaogang Li**[4], and **Robert H. Weiss**[1,2,7]

[1]Division of Nephrology, Dept. of Internal Medicine, University of California, Davis, CA, USA, 95616

[2]Cancer Center, University of California, Davis, CA, USA, 95616

[3]Department of Urology, Shengjing Hospital of China Medical University, 36 Sanhao Street, Shenyang 110004, PR China

[4]Kidney Institute, Dept. of Internal Medicine, University of Kansas Medical Center, Kansas City, KS, USA, 66160

[5]Division of Nephrology, Dept of Medicine, Washington University, St Louis, MO, 63110

[6]Karyopharm Therapeutics, Inc, Newton, MA 02459

[7]Medical Service, Sacramento VA Medical Center, Sacramento, CA, USA, 95655

Abstract

Autosomal Dominant Polycystic Kidney Disease (ADPKD) is a common hereditary renal disease with no current available targeted therapies. Based on the established connection between β-catenin signaling and renal ciliopathies, and on data from our and other laboratories showing striking similarities of this disease and cancer, we evaluated the use of an orally bioavailable small molecule, KPT-9274 (a dual inhibitor of the protein kinase PAK4 and nicotinamide phosphoribosyl transferase), for treatment of ADPKD. Treatment of PKD-derived cells with this compound not only reduces PAK4 steady state protein levels and regulates β-catenin signaling, but also inhibits nicotinamide phosphoribosyl transferase, the rate-limiting enzyme in a key NAD salvage pathway. KPT-9274 can attenuate cellular proliferation and induce apoptosis associated with a decrease in active (phosphorylated) PAK4 and β-catenin in several *PKD1*-null murine cell

Corresponding Author: Dr. Robert H. Weiss, Division of Nephrology, Department of Internal Medicine, Genome and Biomedical Sciences Building, Room 6311, 451 Health Sciences Dr., University of California, Davis, CA. 95616, rhweiss@ucdavis.edu, Tel: 530-752-4010; FAX: 530-752-3791.

STATEMENT OF COMPETING FINANCIAL INTERESTS

W.S. and E.B. are employees of Karyopharm Therapeutics and provided advice but did not influence the experiments or conclusions of the paper. Karyopharm provided KPT-9274 and an unrestricted gift for purchase of some reagents.

lines, with a less pronounced effect on the corresponding phenotypically normal cells. Additionally, KPT-9274 shows inhibition of cytogenesis in an *ex vivo* model of cyclic AMP-induced cystogenesis as well as in the early stage *Pkd1flox/flox:Pkhd1-Cre* mouse model, the latter showing confirmation of specific anti-proliferative, apoptotic and on-target effects. NAD biosynthetic attenuation by KPT-9274, while critical for highly proliferative cancer cells, does not appear to be important in the slower growing cystic epithelial cells during cystogenesis. KPT-9274 was not toxic in our ADPKD animal model or in other cancer models. Thus, this small molecule inhibitor could be evaluated in a clinical trial as a viable therapy of ADPKD.

Keywords

ADPKD; signaling; apoptosis

INTRODUCTION

Autosomal Dominant Polycystic Kidney Disease (ADPKD) is a common hereditary renal disease associated with the formation of fluid filled cysts in the kidney as well as in other epithelial organs including the liver and pancreas[1]. With a prevalence of 1 in 500 – 1000 individuals, it is the most prevalent monogenic disorder in humans and a common cause of end-stage renal disease (ESRD)[2,3]. While there is a great deal known about the signaling defects underlying this disease, an enormous effort to evaluate targetable pathways, and new discoveries frequently added, there are still no ADPKD specific therapies currently available. Efforts in our[4] and other[5,6] laboratories have focused on metabolic reprogramming in PKD which in many cases shows a striking similarity to malignancy. Through conventional principles that drive oncologic research, studies on cyst formation in PKD can lead to re-purposing of effective cancer drugs for use in these patients.

Building on studies in cancer[7–9], we have identified the PAK/WNT/β-catenin signaling as a potential target for PKD. Overexpression of PAKs influence a broad range of cellular activities with involvement in several oncogenic signaling pathways, including cell proliferation and mitogenesis[9], hence their evaluation as potential targets for dysregulated proliferative diseases including renal cystic disease. PAK4, the first of the group II PAKs to be cloned and characterized, is involved with regulating such cyst-promoting events as actin-mediated cell morphology, embryonic development, and cell cycle regulation[10–12]. In addition, deletion of PAK4 reduces tumor formation through inhibition of cell growth[13] and would thus be expected to have similar effects on the dysregulated renal tubular epithelial cell proliferation seen in renal cystic disease.

In this report we investigate the utility of the dual PAK4/NAMPT inhibitor, KPT-9274, (and by inference analogs such as KPT-7523, KPT-8752, and KPT-9331)[14,15] to reduce PAK4 steady state protein levels in PKD. We show here that KPT-9274 treatment, primarily through PAK4 inhibition, causes reduction of cell proliferation and induction of apoptosis in PKD. In addition, administration of KPT-9274 reduces cystogenesis both *ex vivo* and *in vivo* with the expected on-target effects. Based on our data presented in this report, the minimal toxicity of oral administration of KPT-9274 given either for short or long periods in other

animal models[9,16–18] and the fact that KPT-9274 has entered human Phase 1 clinical trials in advanced solid malignancies (NCT02702492), there is strong evidence that this small molecule could be directly evaluated in a clinical trial of ADPKD patients.

RESULTS

KPT-9274 is a potent dual PAK4 and NAMPT inhibitor

KPT-9274 is an orally bioavailable small molecule (Fig. 1a) that shows dual inhibition of PAK4 and NAMPT[9,15,17,18]. When injected into rats, the compound and its acetylated metabolite were found by LC-MS analysis to be present in plasma and bile but undetectable in urine (unpublished observations). Specificity of inhibition of PAK4 by KPT-9274 was previously demonstrated using a CRISPR PAK4 knock out cell line[9,16] and is demonstrated here by a dose-dependent reduction in phosphorylated PAK4 (pPAK4) and total PAK4 in lysates of both postnatal *Pkd1*-null (PN24) and *Pkd1*-heterozygous (PH2; control) cells as well as *Pkd1*-null versus wild-type (wt) control mouse embryonic kidney (MEK) cells, with a more substantial decrease in *Pkd1*-null MEK null cells as compared MEK-wt (Fig. 1b). While likely less important in PKD signaling (*vide infra*) KPT-9274 also shows inhibition of NAMPT (rate-limiting enzyme necessary for NAD biosynthesis) as evidenced by decreased total NAD+NADH levels in both PH2 and PN24 cells with no significant difference between them (Fig. 1c).

KPT-9274 decreases viable cell number through apoptosis and cell cycle arrest

After incubation with KPT-9274 for 72 hours, the viability of PN24 cells was attenuated more markedly than PH2 cells, with an IC_{50} of 2.68 μM for PN24 cells (Fig. 2a); a similar qualitative result was seen with MEK-null compared to MEK-wt cells, with an IC_{50} of 0.469 μM for MEK-null cells. To determine whether KPT-9274 attenuates tubular epithelial cell growth and apoptosis, properties associated with progression of ADPKD[3,19], we demonstrated a dose-dependent decrease in cell proliferation as assessed by methylene blue staining in both sets of cell lines (Fig. 2b), and an increase in apoptosis as determined by Annexin V flow cytometry (Fig. 2c) with both proliferation and apoptosis of both PDK-null cell lines being significantly affected by a lower dose of KPT-9274 compared to their respective normal cell line.

To further evaluate the mechanism of the attenuated cell number seen with KPT-9274 incubation, we quantified the number of cell division events using live-cell imaging. Consistent with the methylene blue data, KPT-9274 was more effective in suppressing cell division events in PN24 cells when compared to PH2 cells by about two fold ($p<0.001$) (Fig. 2d, videos in Supplemental Materials). Thus, KPT-9274 attenuates cell proliferation and decreases cell viability with a predilection for homozygous null ADPKD cells (PN24 and MEK null) as compared to their heterozygous or homozygous normal control cells (PH2 and MEK WT).

KPT-9274 treatment attenuates β-catenin levels without affecting ciliary length and number

Dysregulation of the β-catenin dependent WNT signaling pathway leads to cystic disease[20–22], possibly through disruption of the ciliary signaling machinery[23]. Cilia are

microtubule-based sensory organelles that play a critical role in kidney homeostasis, and it is well established that defects in the assembly or function of cilia cause PKD[24]. However, the mechanism and significance of this interaction is currently unknown. As PAK4 is known to phosphorylate β-catenin (Serine 675)[25] leading to activation of the WNT/β-catenin signaling pathway in both cancer[25] and cystic disease[26], we analyzed the expression levels of β-catenin in cell lysates. We noted a decrease in expression of phosphorylated β-catenin levels in the presence of KPT-9274 in all four cell lines and a decrease in total β-catenin expression in both homozygous null ADPKD lines (PN24, MEK null) and the heterozygous ADPKD line (PH2) (Fig. 3a).

We next explored the influence of KPT-9274 on ciliogenesis in murine inner medullary collecting duct (IMCD3) cells. In contrast to PH2/PN24 and MEK WT/MEK null cells, IMCD3 cells are a widely studied and reliable model of ciliogenesis since they can be consistently induced to form cilia that are representative of those in the normal kidney[27,28]. Analysis of quiescent IMCD3 cells incubated with KPT-9274 showed no change in the fraction of cells that assembled cilia (Fig. 3b), nor in the average length of cilia per cell (Fig. 3c). Moreover, quantification of ciliogenesis in kidney sections from mice treated with KPT-9274 (described in more detail in the subsequent section below) showed no difference in the percentage of cells that assembled cilia *in vivo* (Fig. 3d). Thus, while the WNT signaling cascade is attenuated by KPT-9274, higher concentrations of this compound do not have adverse effects on ciliogenesis, and are therefore less likely to be toxic to normal renal and non-renal ciliated cells.

KPT-9274 inhibits cystogenesis in an *ex vivo* cAMP-cystogenesis model

Metanephric organ cultures have been used to determine whether embryonic kidney tubules can be stimulated to form cysts and as a way to rapidly assess whether various drugs can inhibit or slow cystic progression[29–31]. Under basal culture conditions, *Pkd*-1 wild-type kidneys from embryonic day 13.5 mice grow in size and continue ureteric bud branching and tubule formation over a 4- to 5-day period. Treatment of these kidneys with cyclic AMP (cAMP) analogues (or the cAMP agonist forskolin) can induce the formation of dilated tubules within 1 h, which enlarge over several days and result in dramatically expanded cyst-like structures of proximal tubule and collecting duct origin. Using this organ culture model, we evaluated direct effects of KPT-9274 on cyst growth in the kidney. Treatment of kidneys isolated from embryonic mice at E13.5 and cultured *ex vivo* for up to 4 days with KPT-9274, in the presence of exogenous cAMP, resulted in significant decreases in the fraction of cystic area in a dose-dependent manner (Fig. 4).

Intraperitoneal dosing of KPT-9274 delays cyst growth in Pkd1$^{flox/flox}$:Pkhd1-Cre mice

In light of its inhibition of cancer signaling pathways, many of which we and others have shown to be relevant to ADPKD, we next asked whether KPT-9274 would have a salutary effect on cyst growth in a well-established early-stage ADPKD mouse model[16]. Sixteen *Pkd1$^{flox/flox}$:Pkhd1-Cre* mice were treated intraperitoneally daily with 60 mg/kg of KPT-9274 or vehicle control for 15 days then kidneys were harvested at sacrifice, 24 h after the last dose of KPT-9274. Phosphorylated and total β-catenin were markedly elevated in *Pkd1$^{flox/flox}$:Pkhd1-Cre* mice as compared to *Pkd1$^{+/+}$:Pkhd1-Cre* mice (Fig. 5a) suggesting

basal and constitutive activation of this pathway in PKD. In order to show target specificity of KPT-9274, we performed a separate experiment with *Pkd1*$^{+/+}$*:Pkhd1-Cre* mice treated daily with intraperitoneal KPT-9274 (100 mg/kg) or vehicle, and harvested the kidneys only 16 h after the last dose. It can be seen that total-PAK4 and to a lesser extent total-β-catenin, were decreased in the kidneys from treated animals (Fig. 5b), consistent with target engagement of KPT-9274[17]. In the *Pkd1*$^{flox/flox}$*:Pkhd1-Cre* mice, KPT-9274 treatment resulted in significantly decreased cyst growth, kidney size, and BUN when compared to vehicle treated controls (Fig. 5c–f). Consistent with this data, PCNA staining demonstrated less cell proliferation in KPT-9274 treated mice when compared to vehicle treated controls (Fig. 5f), and more apoptotic cell death in KPT-9274 treated mice was demonstrated by more TUNEL positive epithelial cells lining cysts (Fig. 5g). Thus, KPT-9274 effectively inhibits cyst growth by decreasing cell proliferation in *Pkd1*$^{flox/flox}$*:Pkhd1-Cre* mice, suggesting an attractive therapeutic approach for treatment of at least early stage ADPKD. KPT-9274 treatment did not affect mouse body weight at the conclusion of the experiment (vehicle control: 7.28+/−0.66; KPT-9274 treated: 6.6 +/− 1.0; p=0.13), suggesting a lack of general toxicity.

The NAD salvage pathway is an unlikely mechanism of KPT-9274 in ADPKD

By virtue of its inhibition of NAMPT, KPT-9274 attenuates NAD regeneration through one of the NAD salvage pathways[9]. In normal cells, there exists two salvage pathways for NAD regeneration, but in some cancers[7], including RCC[9,32], the NAD synthetic pathway operates primarily through NAMPT. In RCC, hypermethylation of the NAPRT1 promoter results in downregulation of NAPRT1 mRNA and protein causing rapidly proliferative cancer cells to be highly dependent on NAMPT activity[33] for NAD regeneration and cell survival[34]. To evaluate this requirement in PKD, we show (as expected) that KPT-9274 decreased total NAD+NADH in both PN24 and PH2 cells by a similar magnitude (see Fig. 1c), which argues against any differential requirement in PKD. The lack of change in baseline NAMPT or NAPRT1 levels in these cells support this hypothesis (Fig. 6a).

Furthermore, unlike in the cell lines, the *Pkd1*$^{flox/flox}$*:Pkhd1-Cre* model tissues (Fig. 6b) as well as human PKD tissues (Fig. 6c) showed the opposite changes in NAMPT as are seen in cancer[9], notably lower levels of NAMPT in ADPKD (which regulates the salvage pathway of NAD generation attenuated by KPT-9274). This may explain why KPT-9274 did not significantly decrease total NAD+NADH in kidneys at 24 h after the last administration of KPT-9274 (Fig. 6d): the NAD+NADH level is much lower in the *Pkd1*$^{flox/flox}$*:Pkhd1-Cre* model compared to *Pkd1*$^{+/+}$*:Pkhd1-Cre* kidneys, perhaps as a result of decreased NAMPT expression (Fig. 6d). Taken together, these data suggest that, unlike rapidly proliferating cancer cells, PKD epithelial cells are not dependent on a high and readily available sink of NAD, and KPT-9274 is not decreasing cystogenesis through this pathway in PKD cells and has greater dependence on the PAK4/WNT signaling pathway. However, it remains possible that KPT-9274 retains an inhibitory effect on systemic NAMPT in patients, and thus it may limit NAD availability in PKD tissue. Further investigations of this possibility would need to occur before clinical translation of KPT-9274 to ADPKD in order to determine the potential need for nicotinic acid supplementation.

DISCUSSION

Although postulated originally by Grantham in 1990 to be a “neoplasm in disguise”[35], the similarities between ADPKD and cancer have only lately been revisited[4,36]. In recent years, there has been increasing evidence demonstrating the utility of investigating these parallels such that available cancer drugs can be repurposed to treat ADPKD[4–6]. It should not be surprising that these drugs work in light of the fact that there are many metabolic pathways shared between cancer and cystic disease which have been associated with epithelial proliferation, cell death pathways, and consequent cyst formation in ADPKD. For example, defects in renal ciliary signaling leading to aberrant epithelial cell proliferation have long been known to contribute to cystogenesis[37], such that targeting these pathways, as we have done here with the PAK4/WNT/β-catenin axis, has been a promising area of research and potential therapeutic intervention.

While mutations in *PKD1* or *PKD2*[38,39] lead ultimately to translation of transmembrane proteins which co-localize to the renal cilium presumably to monitor environmental cues[38], cystic diseases have also been linked to defective WNT/β-catenin signaling[19–21], a well-known oncogenic pathway regulated by the p21 activated kinase (PAK) family[7] of serine/threonine kinases[25]. Specifically, mice exposed to constitutively active β-catenin develop severe cystic kidney disease[21]. Here, we demonstrate specific and effective use of a PAK4 inhibitor, KPT-9274, that decreases cell viability and proliferation and increases apoptosis in PH2 and PN24 cells. Furthermore, KPT-9274 treatment leads to cell cycle arrest and apoptosis in ADPKD cells. This effect is likely mediated through β-catenin inhibition resulting in a blockade to cyst formation and growth in both the *ex vivo* cAMP cystogenesis model as well as the early stage mouse model of ADPKD. Importantly, we did not observe a KPT-9274-dependent effect on ciliogenesis, demonstrating a lack of KPT-9274 impact on cilia assembly in normal quiescent non-dividing cells, a concept consistent with our *in vivo* results described here, as well as results from us[9] and other investigators who have administered KPT-9274 to animals for variable times[16–18]. This is promising and suggests that future KPT-9274 clinical trials may have a positive therapeutic effect on individuals with ADPKD without adverse effects.

In addition to PAK4, KPT-9274 impacts NAD biosynthesis through binding/inhibiting the rate-limiting enzymes, NAMPT, which mediates a crucial energy requirement in rapidly growing cells typified in cancer[7] including RCC[9]. This aspect of KPT-9274 biochemistry most likely plays a smaller role in the PKD models since these cells and tissues are able to synthesize or obtain NAD through NAPRT1[7] salvage pathway (see Fig. 6b) at a rate not limited by the rapid cell growth seen in cancer cells and tissues. Since NAPRT1 utilizes exogenous niacin (nicotinic acid) to make NAD, co-dosing KPT-9274 with niacin may further alleviate any risk of toxicity by inhibition of NAMPT for the treatment of ADPKD[7,9].

Our findings are strengthened by validation of the salutary effects of KPT-9274 in an established cAMP-induced *ex vivo* cystogenesis model for ADPKD. Treatment with 20 μM of KPT-9274 decreased cystic area by approximately 50% in the *ex vivo* model, which is similar to that seen in the *in vivo* experiments. Thus, confirmation of an anti-cystic effect in

several separate models of ADPKD, *in vitro, ex vivo*, and *in vivo*, strengthens our conclusions regarding the potential utility of this inhibitor for treatment of the human disease. Research from our laboratory showed that when KPT-9274 was orally administered to a 786-O (VHL-mut) human RCC xenograft model, there was dose-dependent inhibition of tumor growth with minimal toxicity[9], data which is in line with several other recent publications from other institutions when KPT-9274 was administered both intravenously[18] and orally[16,17], the latter up to 42 days[17]. Currently, KPT-9274 is being evaluated in a Phase 1 human clinical trial in patients with advanced solid malignancies or NHL (NCT02702492), thus there have been toxicity studies performed in a variety of animal models that allowed initiation of this clinical study. Furthermore, data from this clinical trial will allow the data presented in this report, as well as on RCC, to be rapidly translated into the clinic for the treatment of both kidney diseases.

In conclusion, we demonstrate potent inhibition of PKD models with a dual PAK4/NAMPT inhibitor, KPT-9274. We show KPT-9274 slows cyst formation and growth in several models of cystogenesis and ADPKD likely through inhibition of PAK4 and the downstream effector, β-catenin, important in cystogenesis. Given the lack of toxicity of this compound presented here and by others, our work suggests a new approach for treatment of renal cystic disease by selectively blocking PAK4 mediated pathways.

CONCISE METHODS

Cellular Assays

Postnatal PKD1 heterozygous (PH2) and PKD1 homozygous null (PN24) cells were of proximal tubule origin and cultured as described[40] (provided by S. Somlo through the George M O'Brien Kidney Center, Yale University, New Haven, Connecticut, USA). MEK-wt and MEK-null cells were cultured as previously described[41]. KPT-9274 was re-suspended in DMSO and aliquoted at 10 mM and kept in the dark. Cells were treated with various concentrations of KPT-9274 for 72 h before analysis by MTT. IC_{50} values were calculated using a four parameter curve fit (Graphpad Prism). MTT assays were performed as described previously[42]. Briefly cells were treated with MTT and assayed after 3 h. Visible absorbance of each well was quantified at 570 nm using a microplate reader. For quantification of apoptosis, cells were stained using the Annexin V kit (Millipore) and analyzed on the Muse Cell Analyzer from Millipore (Billerica, MA) following the manufacturer's instructions. Triplicate samples were used to obtain the mean and standard deviation and student's t-tests were performed. For methylene blue assays[43], cells were stained with methylene blue for 30 min and quantified at 665 nm on a microplate reader after washing.

Immunoblotting

Immunoblotting was performed as previously described[42]. Briefly, cells were treated with various concentrations of KPT-9274 (0.625, 2.5, and 10 μM) for 24 h and lysed with RIPA lysis buffer (Thermo Scientific) before immunoblotting. Tissues were homogenized in T-PER buffer (Thermo Scientific). Membranes were blocked in 5% BSA or Odyssey Blocking buffer (LI-COR) for one hour at room temperature and probed with appropriate primary and

secondary antibodies. Signal was detected with ECL using the Fuji Imager or with fluorescent secondary antibodies (LI-COR) using Odyssey. β-catenin, phospho-β-catenin, PAK4, phospho-PAK4 and vinculin antibodies were from Cell Signaling and probed at 1:1000. β-actin (Sigma) was probed at 1:4000, NAMPT (Bethyl Laboratories) was probed at 1:2000, and NAPRT1 (Proteintech) was probed at 1:2000. Image J (https://imagej.nih.gov/) was used to measure densitometry.

Live Cell Imaging

PH2 and PN24 cells were cultured in 12-well plates, seeded at a density of 6×10^4 cells/mL. The next day, medium was supplemented with 10 μM KPT-9274, while control samples received DMSO only as vehicle control. Cells were maintained on the microscope imaging stage at 5% CO_2 and 33°C for up to 72 h. Images were captured at 10 min intervals using a Nikon Eclipse Ti-E inverted confocal microscope equipped with a 10× Phase objective lens (Nikon). The number of cell division events in each sample was quantified using the Object Tracking module of the Nikon Elements AR 4.20 Software. Linear regression was performed by SAS.

Cilia Growth Assays

Inner medullary collecting duct (IMCD3) cells were grown in DMEM medium (Corning) supplemented with 10% FBS (Atlanta Biologicals) and 1% penicillin-streptomycin (Gibco). To induce primary cilium formation, cells were arrested in G_0 by incubation in DMEM supplemented with 0.5% FBS, with or without 10 μM KPT-9274. Cells were fixed with 4% paraformaldehyde (Electron Microscopy Sciences) in PBS at room temperature for 10 min, permeabilized by washing three times with 0.1% Triton X-100 in PBS (PBS-T), and blocked for 1 h at room temperature with PBS-T supplemented with 3% BSA. Cells were incubated with mouse anti-acetylated tubulin (clone 6-11b-1; 1:10,000; Sigma-Aldrich) and rat anti-ZO-1 (R40.76, 1:1000, Santa Cruz Biotechnology) for 1 h at room temperature, followed by 3 washes for 5 min each in PBS-T. Alexa Fluor dye–conjugated secondary antibodies (Life Sciences) were used at a dilution of 1:500 at room temperature for 1 h. Coverslips were mounted on glass slides using Mowiol mounting medium containing N-propyl gallate (Sigma). Images were captured using a Nikon Eclipse Ti-E inverted confocal microscope equipped with a 100× (1.45 NA) Plan Fluor oil immersion objective lens (Nikon). Quantification of cilia abundance and length was performed using NIS-Elements AR 4.20 software (Nikon). At least 100 cells were scored in three independent experiments (n = 300 cells total per sample).

Ex Vivo kidney organ cultures

Ex vivo cystogenesis assay was performed as previously described[30,31]. Briefly, metanephroi were dissected from embryonic mice at E13.5 and placed on transparent Transwell cell culture inserts (Corning). DMEM/F12-defined culture medium (supplemented with 2 mM L-glutamine, 15 mM HEPES, 5 μg/ml transferrin, 10 μM sodium selenite and 10 μM prostaglandin E1; all from Sigma) was added to the basal chamber, and organ cultures maintained in a 37°C humidified CO_2 incubator for up to 4 days. To induce cystogenesis, the culture medium was supplemented with 100 μM 8-bromoadenosine 3′,5′-cyclic monophosphate (8-Br-cAMP, Sigma) together with either 0, 5, 10 or 20 μM KPT-9274, and

the medium was changed daily. Kidneys were imaged every 24 h for 4 days using a 2× or 4× objective. Quantification of kidney size and cystic area was performed using NIS-Elements AR 4.20 software (Nikon). Fractional cyst area was calculated as total tubule dilation area divided by total kidney area. Four kidneys were analyzed per experimental sample.

Mouse strain and treatment

All animal protocols were approved and conducted in accordance with Laboratory Animal Resources of University of Kansas Medical Center and Institutional Animal Care and Use Committee regulations. *Pkd1*$^{flox/flox}$*:Pkhd1-Cre* mice[40] were generated by cross-breeding *Pkd1*$^{flox/+}$*:Pkhd1-Cre* female mice with *Pkd1*$^{flox/+}$*:Pkhd1-Cre* male mice. *Pkd1*$^{flox/flox}$*:Pkhd1-Cre* neonate was intraperitoneally injected daily with KPT-9274 (60 mg/kg) or vehicle control from postnatal day 10 (PN10) to postnatal day 24 (PN24). All the kidneys were harvested and analyzed at postnatal day 25. Mouse kidneys were placed on dry ice immediately after dissection and weighing.

To examine the effect of KPT-9274 on Pak4 and β-catenin expression *in vivo*, 8 week old *Pkd1*$^{flox/+}$*:Pkhd1-Cre* female mice (n=6) were treated with KPT-9274 (100 mg/kg IP daily) or vehicle for 7 days. The mice were sacrificed 16 h after the last dose of KPT-9274.

Assay of total NAD

PH2 and PN24 cells were plated at 50% confluence and treated with various doses of KPT-9274 for 24 h. Total NAD+NADH was quantified in cell and tissue extracts using the NAD/NADH Glo Assay kit (Promega) following manufacturer's instructions, as we have previously reported[9]. Students t-tests were used for statistical analyses.

Immunohistochemistry

Kidneys were fixed with 4% paraformaldehyde (pH 7.4). The kidney sections were stained by a monoclonal mouse anti-PCNA antibody (Cell Signaling Technologies, 1:1000 dilution), a biotinylated secondary antibody (Sigma, 1:100 dilution), and DAB (3, 3′-diaminabenzidine tetrahydrochloride) substrate system as described previously[44]. The kidney sections were counterstained by haematoxylin. Images were obtained with a NIKON ECLIPSE 80i Microscope. For analysis of ciliogenesis, sections were stained with anti-acetylated tubulin antibody as described above, and the percentage of cells that formed cilia quantified.

TUNEL (terminal deoxynucleotidyl transferase-mediated dUTP nick end-labeling) assay

TUNEL assays for kidneys treated with KPT-9274 or vehicle control was performed according to the manufacturer's protocols (In Situ Death Detection Kit; Roche). Prolong Gold Anti-fade reagent with DAPI (Invitrogen) was used. Immunofluorescence images were obtained with a NIKON ECLIPSE 80i microscope.

Supplementary Material

Refer to Web version on PubMed Central for supplementary material.

Acknowledgments

We thank Mr. Ken Chmiel with his technical help on this manuscript. We thank the O'Brien Kidney Center at Yale (DK079310) for supplying the PH2 and PN24 cells and the MEK WT and MEK null cells. This work was supported by NIH grants 1R01CA135401-01A1, 1R03CA181837-01, and 1R01DK082690-01A1, the Medical Service of the US Department of Veterans' Affairs, and Dialysis Clinics, Inc. (DCI) (all to R.H.Weiss); NIDDK grant 1R01DK108005-01 to M.R. Mahjoub; and NIH grants R01DK084097 and P30DK106912 (all to X. Li). A non-restricted gift for research purposes was provided by Karyopharm, Inc.

References

1. Gabow PA. Autosomal dominant polycystic kidney disease. N Engl J Med. 1993; 329(5):332–342. [PubMed: 8321262]
2. Torres VE, Harris PC, Pirson Y. Autosomal dominant polycystic kidney disease. Lancet. 2007; 369(9569):1287–1301. [PubMed: 17434405]
3. Gabow PA, Johnson AM, Kaehny WD, et al. Factors affecting the progression of renal disease in autosomal-dominant polycystic kidney disease. Kidney Int. 1992; 41(5):1311–1319. [PubMed: 1614046]
4. Hwang VJ, Kim J, Rand A, et al. The cpk model of recessive PKD shows glutamine dependence associated with the production of the oncometabolite 2-hydroxyglutarate. AmJPhysiol Renal Physiol. 2015; 309(6):F492–F498.
5. Rowe I, Chiaravalli M, Mannella V, et al. Defective glucose metabolism in polycystic kidney disease identifies a new therapeutic strategy. NatMed. 2013; 19(4):488–493.
6. Riwanto M, Kapoor S, Rodriguez D, Edenhofer I, Segerer S, Wuthrich RP. Inhibition of Aerobic Glycolysis Attenuates Disease Progression in Polycystic Kidney Disease. PLoSOne. 2016; 11(1):e0146654.
7. Sampath D, Zabka TS, Misner DL, O'Brien T, Dragovich PS. Inhibition of nicotinamide phosphoribosyltransferase (NAMPT) as a therapeutic strategy in cancer. PharmacolTher. 2015; 151:16–31.
8. Dart AE, Wells CM. P21-activated kinase 4–not just one of the PAK. EurJ Cell Biol. 2013; 92(4–5): 129–138. [PubMed: 23642861]
9. Abu Aboud O, Chen CH, Senapedis W, Baloglu E, Argueta C, Weiss RH. Dual and specific inhibition of NAMPT and PAK4 by KPT-9274 decreases kidney cancer growth. MolCancer Ther. 2016
10. Nekrasova T, Minden A. PAK4 is required for regulation of the cell-cycle regulatory protein p21, and for control of cell-cycle progression. J Cell Biochem. 2011; 112(7):1795–1806. [PubMed: 21381077]
11. Abo A, Qu J, Cammarano MS, et al. PAK4, a novel effector for Cdc42Hs, is implicated in the reorganization of the actin cytoskeleton and in the formation of filopodia. EMBO J. 1998; 17(22): 6527–6540. [PubMed: 9822598]
12. Qu J, Li X, Novitch BG, et al. PAK4 kinase is essential for embryonic viability and for proper neuronal development. MolCell Biol. 2003; 23(20):7122–7133.
13. Liu Y, Xiao H, Tian Y, et al. The pak4 protein kinase plays a key role in cell survival and tumorigenesis in athymic mice. MolCancer Res. 2008; 6(7):1215–1224.
14. Senapedis W, Crochiere M, Baloglu E, Landesman Y. Therapeutic Potential of Targeting PAK Signaling. Anticancer Agents MedChem. 2015; 16(1):75–88.
15. Jiang YY, Lin DC, Mayakonda A, et al. Targeting super-enhancer-associated oncogenes in oesophageal squamous cell carcinoma. Gut. 2016
16. Fulciniti M, J M-L, Senapedis W, Oliva S, Bandi R, Amodio N, Xu Y, Szalat RI, Gulla A, Samur MK, Roccaro A, Linares M, Cea M, Baloglu E, Argueta C, Landesman Y, Shacham S, Liu Siyuan, Schenone M, Wu S-L, Karger B, Prabhala R, Anderson KC, Munshi NC. Functional role and therapeutic targeting of p21-associated kinase 4 (PAK4) in Multiple Myeloma. Blood. 2017
17. Rane C, S W, Baloglu E, Landesman Y, Crochiere M, Das-Gupta S, Minden A. A novel orally bioavailable compound KPT-9274 inhibits PAK4 and blocks triple negative breast cancer tumor growth. Scientific Reports. 2017

18. Aboukameel A, Muqbil I, Senapedis W, et al. Novel p21-Activated Kinase 4 (PAK4) Allosteric Modulators Overcome Drug Resistance and Stemness in Pancreatic Ductal Adenocarcinoma. Molecular cancer therapeutics. 2017; 16(1):76–87. [PubMed: 28062705]
19. Ali SM, Wong VY, Kikly K, et al. Apoptosis in polycystic kidney disease: involvement of caspases. AmJ Physiol RegulIntegrComp Physiol. 2000; 278(3):R763–R769.
20. Kim E, Arnould T, Sellin LK, et al. The polycystic kidney disease 1 gene product modulates Wnt signaling. J BiolChem. 1999; 274(8):4947–4953.
21. Saadi-Kheddouci S, Berrebi D, Romagnolo B, et al. Early development of polycystic kidney disease in transgenic mice expressing an activated mutant of the beta-catenin gene. Oncogene. 2001; 20(42):5972–5981. [PubMed: 11593404]
22. Qian CN, Knol J, Igarashi P, et al. Cystic renal neoplasia following conditional inactivation of apc in mouse renal tubular epithelium. J BiolChem. 2005; 280(5):3938–3945.
23. Simons M, Gloy J, Ganner A, et al. Inversin, the gene product mutated in nephronophthisis type II, functions as a molecular switch between Wnt signaling pathways. NatGenet. 2005; 37(5):537–543.
24. Pan J, Seeger-Nukpezah T, Golemis EA. The role of the cilium in normal and abnormal cell cycles: emphasis on renal cystic pathologies. Cell MolLife Sci. 2013; 70(11):1849–1874.
25. Li Y, Shao Y, Tong Y, et al. Nucleo-cytoplasmic shuttling of PAK4 modulates beta-catenin intracellular translocation and signaling. BiochimBiophysActa. 2012; 1823(2):465–475.
26. Wuebken A, Schmidt-Ott KM. WNT/beta-catenin signaling in polycystic kidney disease. Kidney Int. 2011; 80(2):135–138. [PubMed: 21720305]
27. Sang L, Miller JJ, Corbit KC, et al. Mapping the NPHP-JBTS-MKS protein network reveals ciliopathy disease genes and pathways. Cell. 2011; 145(4):513–528. [PubMed: 21565611]
28. Mahjoub MR, Stearns T. Supernumerary centrosomes nucleate extra cilia and compromise primary cilium signaling. CurrBiol. 2012; 22(17):1628–1634.
29. Avner ED. Epithelial polarity and differentiation in polycystic kidney disease. J Cell SciSuppl. 1993; 17:217–222.
30. Magenheimer BS, St John PL, Isom KS, et al. Early embryonic renal tubules of wild-type and polycystic kidney disease kidneys respond to cAMP stimulation with cystic fibrosis transmembrane conductance regulator/Na(+),K(+),2Cl(−) Co-transporter-dependent cystic dilation. J AmSoc Nephrol. 2006; 17(12):3424–3437.
31. Anders C, Ashton N, Ranjzad P, Dilworth MR, Woolf AS. Ex vivo modeling of chemical synergy in prenatal kidney cystogenesis. PLoS One. 2013; 8(3):e57797. [PubMed: 23554868]
32. Wettersten HI, Hakimi AA, Morin D, et al. Grade-dependent metabolic reprogramming in kidney cancer revealed by combined proteomics and metabolomics analysis. Cancer Res. 2015; 75(12): 2541–2552. [PubMed: 25952651]
33. Kirkland JB. Niacin status, NAD distribution and ADP-ribose metabolism. Curr Pharm Des. 2009; 15(1):3–11. [PubMed: 19149597]
34. Watson M, Roulston A, Belec L, et al. The small molecule GMX1778 is a potent inhibitor of NAD + biosynthesis: strategy for enhanced therapy in nicotinic acid phosphoribosyltransferase 1-deficient tumors. Mol Cell Biol. 2009; 29(21):5872–5888. [PubMed: 19703994]
35. Grantham JJ. Polycystic kidney disease: neoplasia in disguise. Am J Kidney Dis. 1990; 15(2):110–116. [PubMed: 2405652]
36. Seeger-Nukpezah T, Geynisman DM, Nikonova AS, Benzing T, Golemis EA. The hallmarks of cancer: relevance to the pathogenesis of polycystic kidney disease. Nat Rev Nephrol. 2015
37. Pazour GJ. Intraflagellar transport and cilia-dependent renal disease: the ciliary hypothesis of polycystic kidney disease. J Am Soc Nephrol. 2004; 15(10):2528–2536. [PubMed: 15466257]
38. Bycroft M, Bateman A, Clarke J, et al. The structure of a PKD domain from polycystin-1: implications for polycystic kidney disease. EMBO J. 1999; 18(2):297–305. [PubMed: 9889186]
39. Mochizuki T, Wu G, Hayashi T, et al. PKD2, a gene for polycystic kidney disease that encodes an integral membrane protein. Science (New York, NY). 1996; 272(5266):1339–1342.
40. Shibazaki S, Yu Z, Nishio S, et al. Cyst formation and activation of the extracellular regulated kinase pathway after kidney specific inactivation of Pkd1. Hum Mol Genet. 2008; 17(11):1505–1516. [PubMed: 18263604]

41. Zhou X, Fan LX, Sweeney WE Jr, Denu JM, Avner ED, Li X. Sirtuin 1 inhibition delays cyst formation in autosomal-dominant polycystic kidney disease. J Clin Invest. 2013; 123(7):3084–3098. [PubMed: 23778143]

42. Inoue H, Hwang SH, Wecksler AT, Hammock BD, Weiss RH. Sorafenib attenuates p21 in kidney cancer cells and augments cell death in combination with DNA-damaging chemotherapy. Cancer Biol Ther. 2011; 12(9)

43. Byrne KM, C X, Vierck J, Erickson S, Green EA, Duckett S, Dodson MV. Use of a 96-well plate reader to evaluate proliferation of equine satellite cell clones in vitro. Methods Cell Sci. 1998; 19:311–316.

44. Zhou X, Fan LX, Peters DJ, Trudel M, Bradner JE, Li X. Therapeutic targeting of BET bromodomain protein, Brd4, delays cyst growth in ADPKD. HumMolGenet. 2015; 24(14):3982–3993.

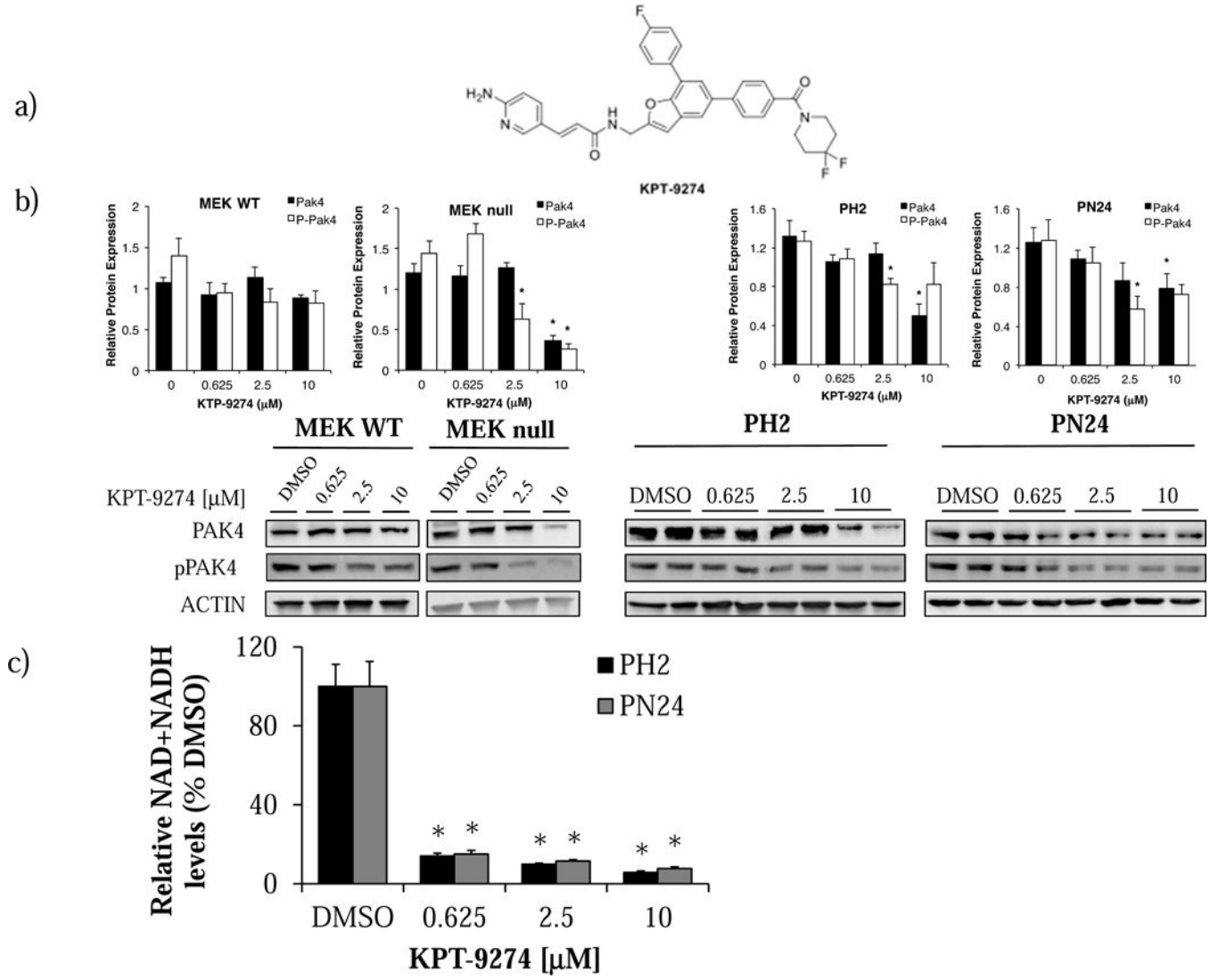

FIGURE 1.

KPT-9274 is a dual inhibitor of PAK4 and NAMPT.

(a) The structure of KPT-9274.

(b) PH2, PN24, MEK WT, and MEK null cells were grown to 50% confluence and treated for 24 h with KPT-9274. Subsequently the indicated cells were lysed and subjected to immunoblotting for total and phosphorylated (Serine 474) PAK4; β-actin was used as a loading control. Image J quantification of protein expression corrected for β-actin is above the blots. Data are means ± SEM (n=3–6).

(c) Total NAD+NADH levels were measured in cells treated with different concentrations of KPT-9274 for 24h as described in Materials and Methods. *$p<0.05$ as compared to DMSO (vehicle) control. Data are means ± SD (n=3).

Experiments shown are representative of at least three repeats

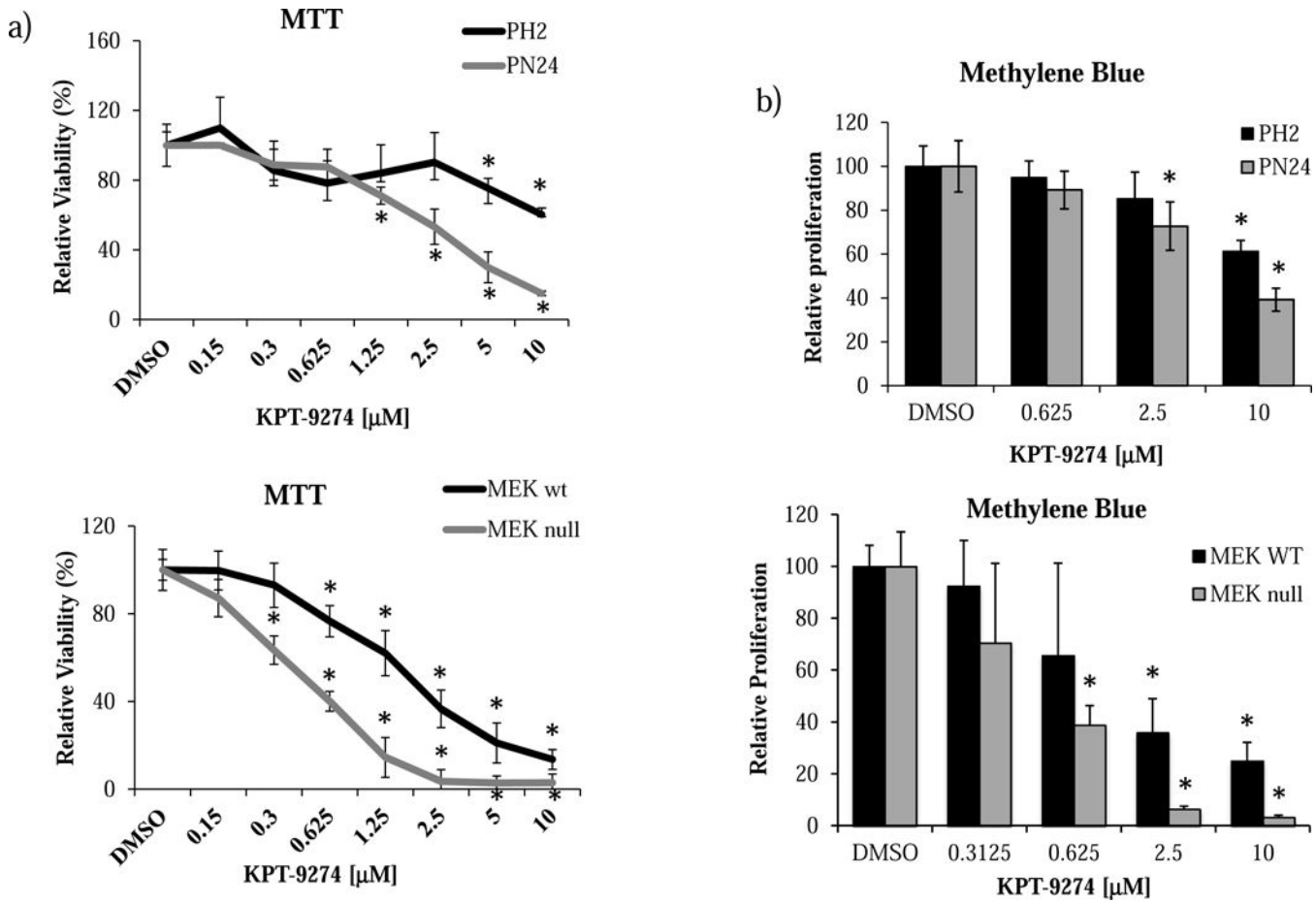

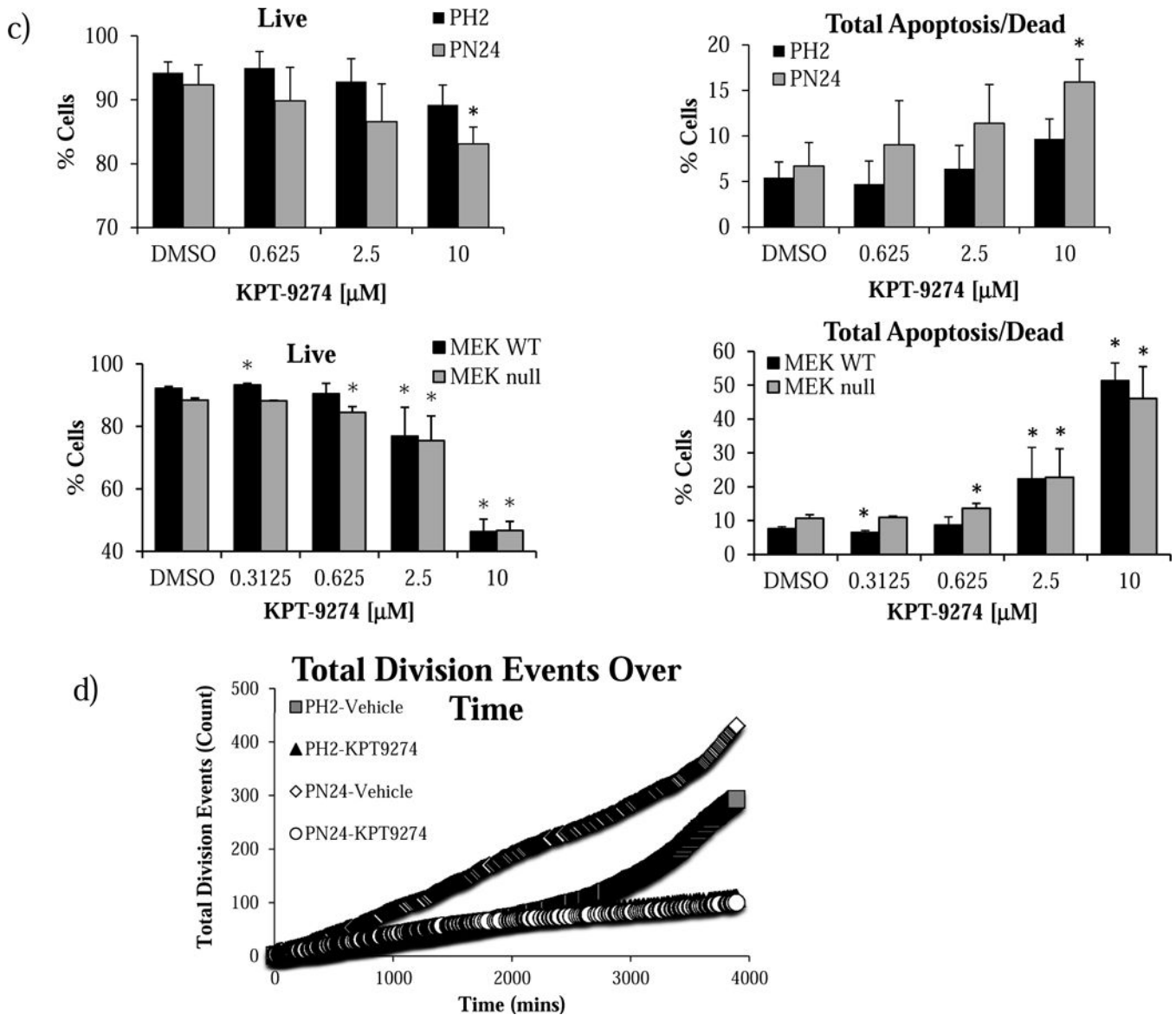

FIGURE 2.

KPT-9274 results in cell death through apoptosis and cell cycle arrest.

PH2, PN24, MEK-wt, and MEK-null cells were grown to 50% confluence and treated with KPT-9274 for 72h at the concentrations indicated and subjected to (a) MTT assay, (b) methylene blue assay, (c) Annexin V staining by flow cytometry, and (d) total cell division events were measured over 4000 min using live-cell imaging (see Materials and Methods). *$p<0.05$ as compared to DMSO (vehicle) control. Experiments shown are representative of at least three repeats except for (d) which was performed twice. Data are means ± SD.

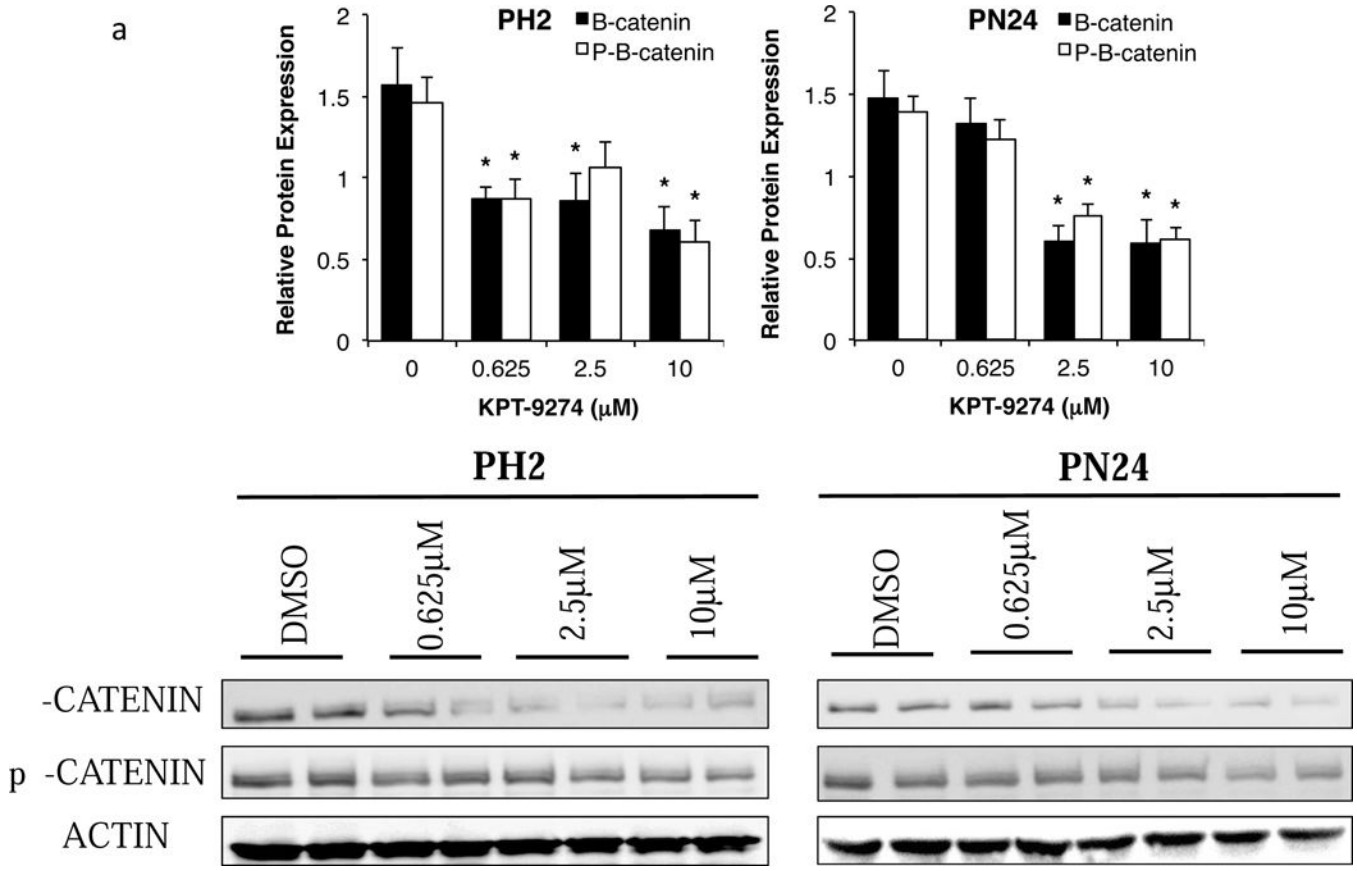

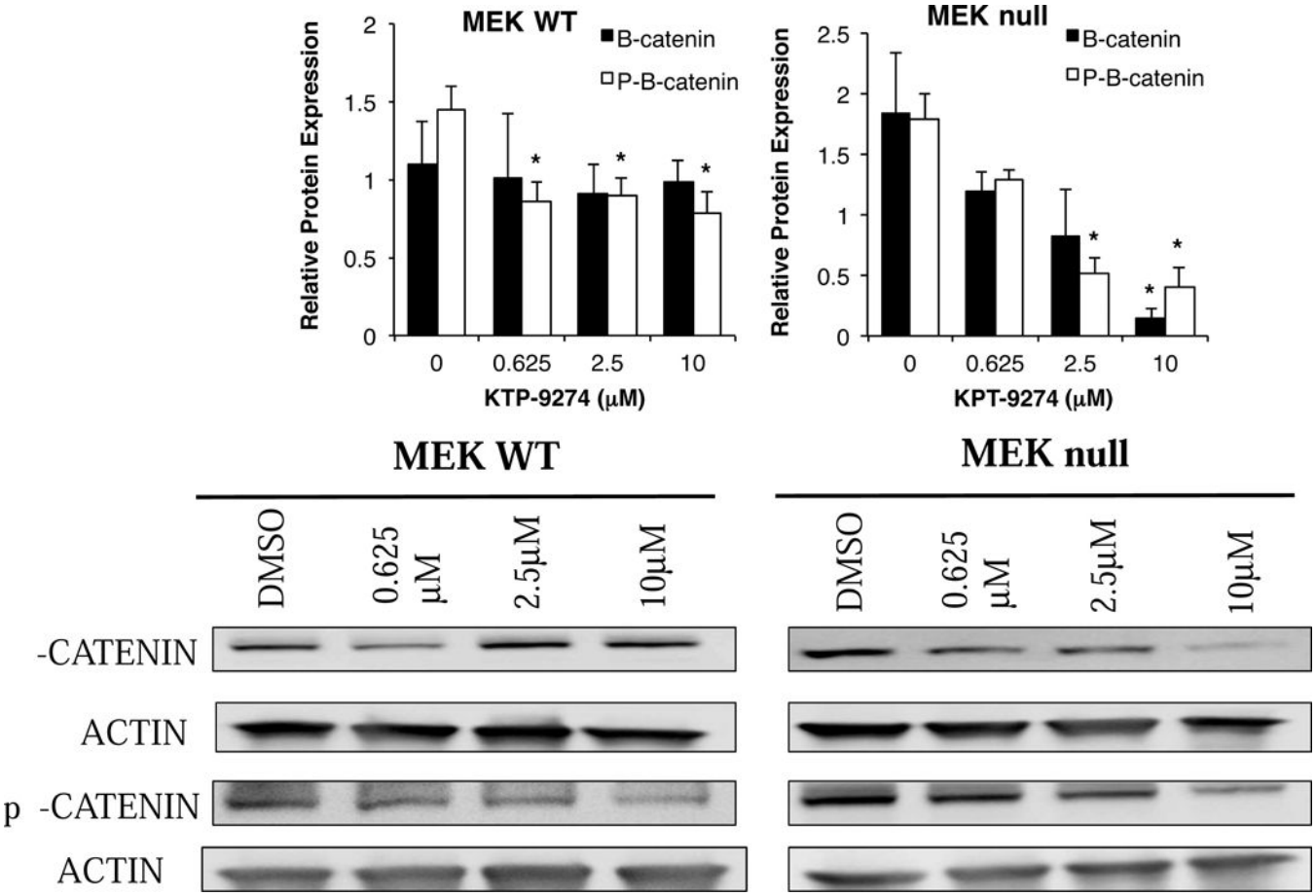

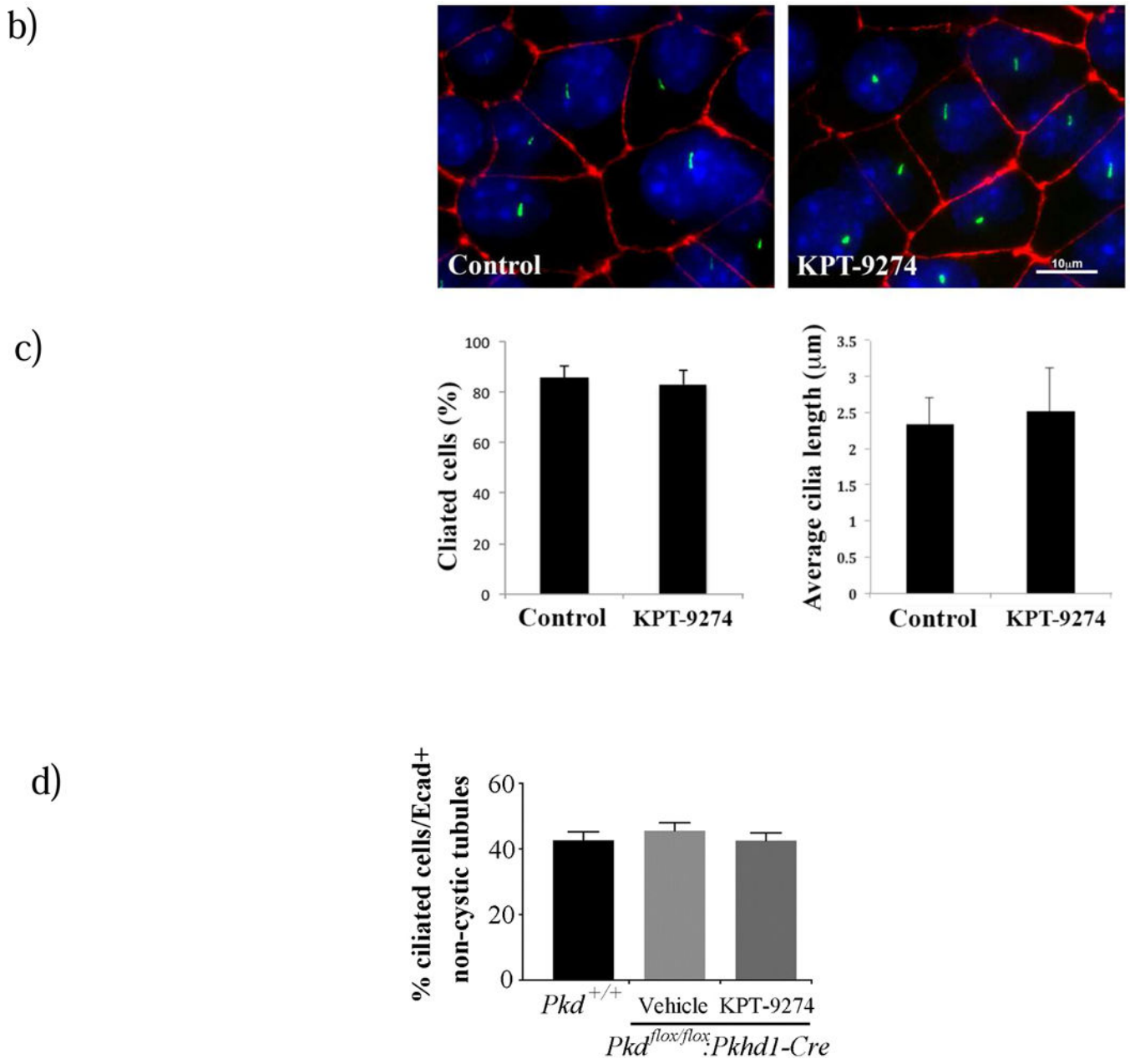

FIGURE 3.

KPT-9274 treatment disrupts β-catenin levels but does not affect ciliary length and number. (a) PH2 and PN24 cells and MEK-wt and MEK-null cells were grown to 50% confluence, treated with KPT-9274 for 24 h at the concentrations indicated and subjected to immunoblotting with total and phosphorylated (Serine 675) β-catenin antibodies. Experiments shown are representative of at least three repeats. Image J quantification of protein expression corrected for β-actin is above the blots. Data are means ± SEM (n=3–6). (b) IMCD3 cells were grown to confluence and serum-starved for 72 h to induce ciliogenesis in the presence of 10 μM KPT-9274. Cells were fixed and immunostained with antibodies against acetylated tubulin to mark cilia (green), ZO-1 to highlight cell-cell junctions (red)

and DNA (DAPI, blue). (c) Quantification of ciliogenesis and ciliary length in KPT-9274-treated IMCD3 cells. Data are means ± SD. N = 300 cells for each sample, from 3 independent experiments. (d) Analysis of ciliogenesis in KPT-9274-treated mice. Kidney sections from wild-type ($Pkd^{+/+}$), untreated *Pkd1*$^{flox/flox}$*:Pkhd1-Cre* (vehicle) and KPT-9274-treated *Pkd1*$^{flox/flox}$*:Pkhd1-Cre* (KPT-9274) mice were immunostained with antibodies against acetylated tubulin to mark cilia, and the percentage of ciliated cells determined. N = 286 cells from 59 tubules scored (wild-type), 321 cells from 52 tubules (*Pkd1*$^{flox/flox}$ vehicle), and 427 cells from 67 tubules (*Pkd1*$^{flox/flox}$ KPT-9274). Data are means ± SD.

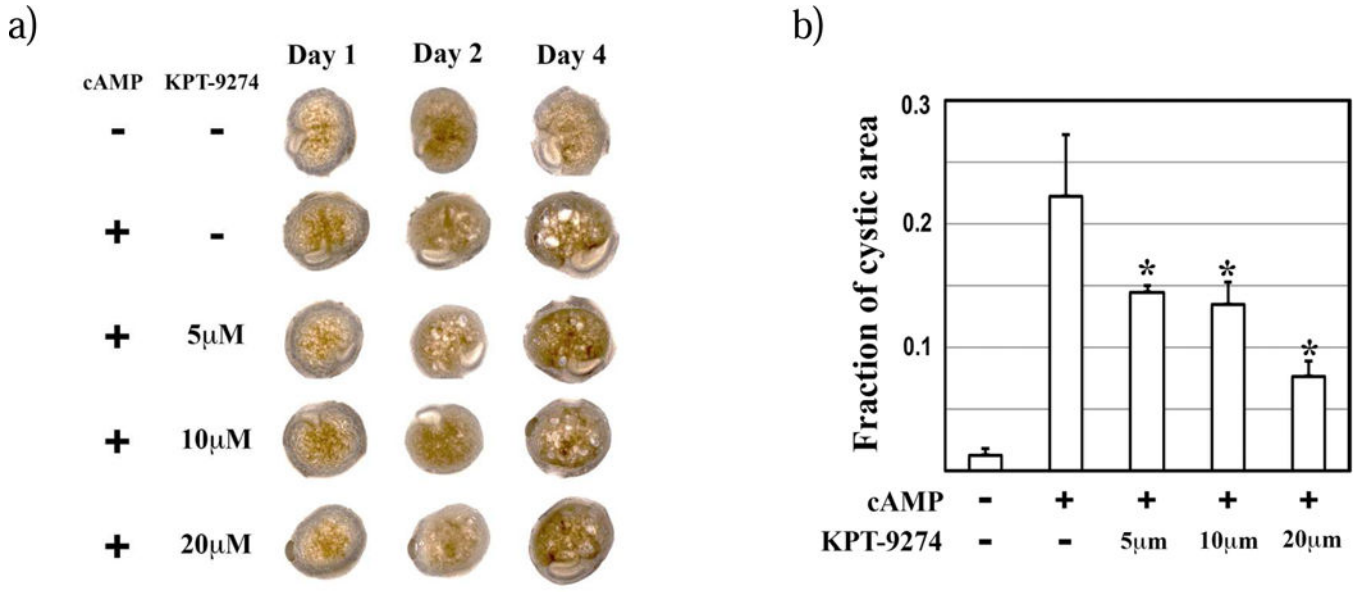

FIGURE 4.

KPT-9274 attenuates cAMP-induced cystogenesis in *ex vivo* kidney organ cultures. Embryonic kidneys were harvested from CD1 mice at E13.5 and cultured *ex vivo* on Transwell membranes for 4 days. Samples were treated with 100 μM 8-Br-cAMP and increasing concentration of KPT-9274.

(a) Images of kidneys taken on days 1–4, showing cystic progression.

(b) Quantification of fractional cyst area in control and treated kidneys at day 4. Cystogenesis was quantified by dividing the cystic area by the total area of each kidney. N = 4 kidneys per sample *$p<0.05$ as compared to DMSO (vehicle). Data are means ± SD.

a)

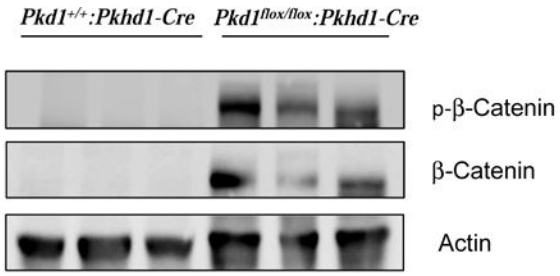

b)

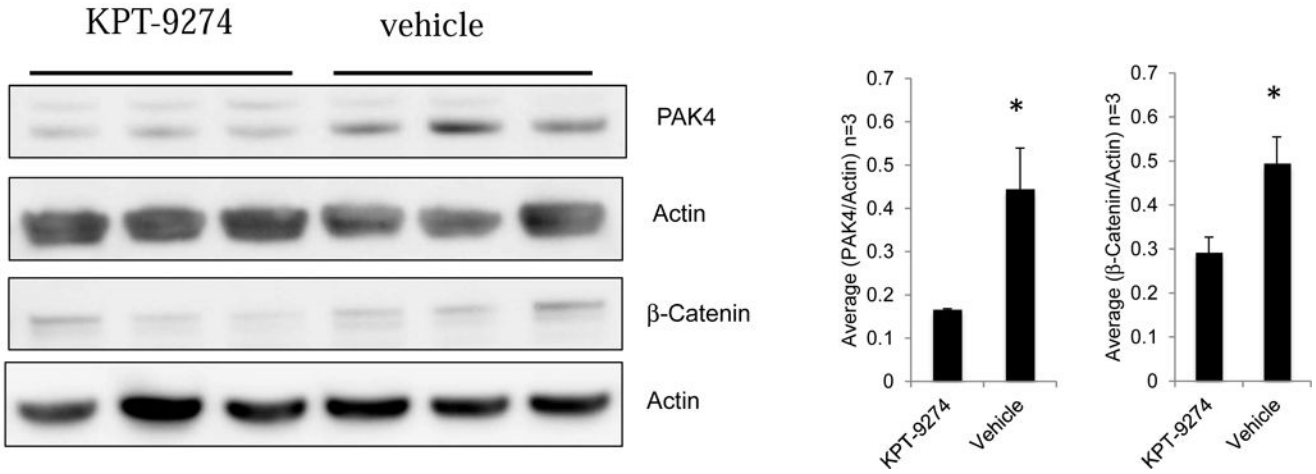

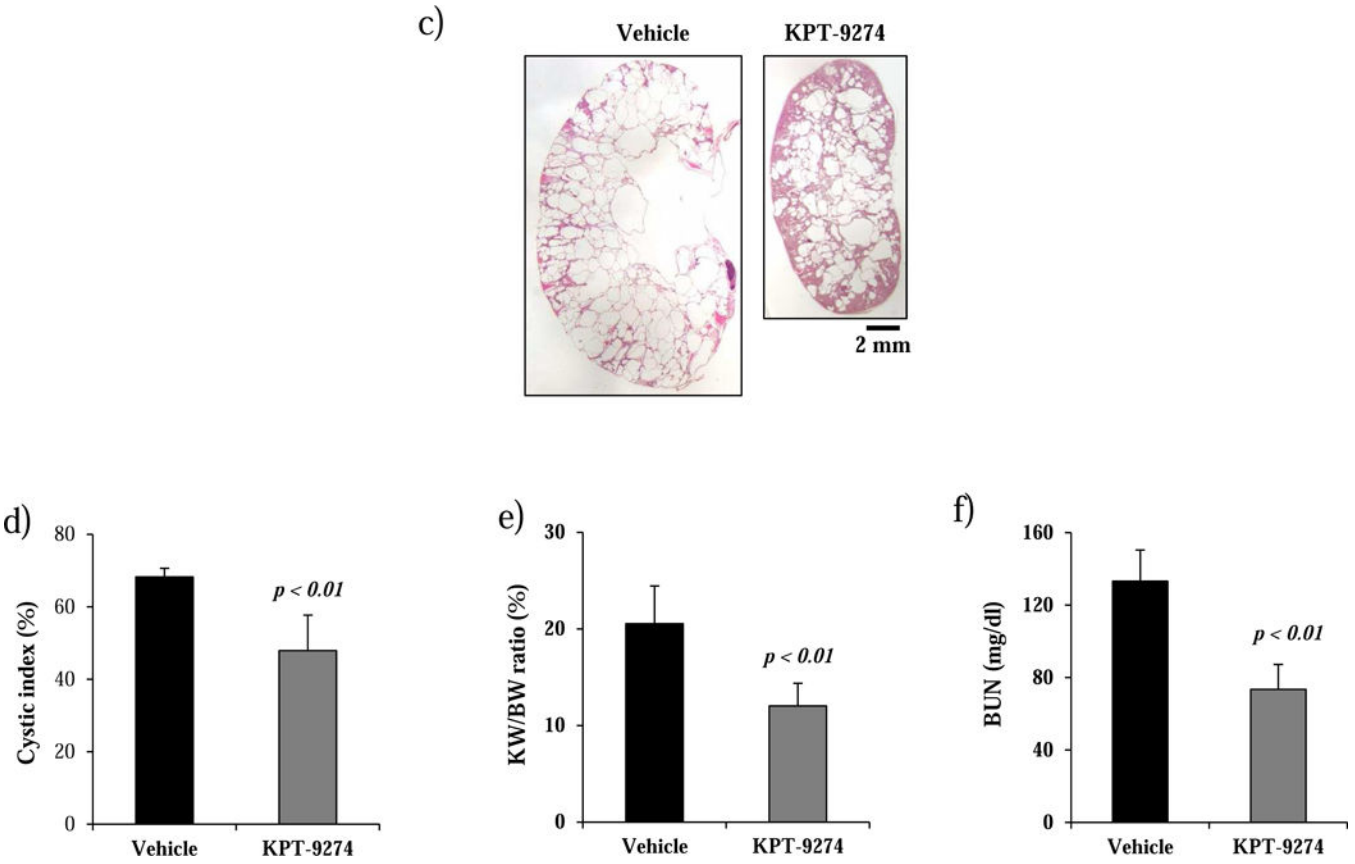

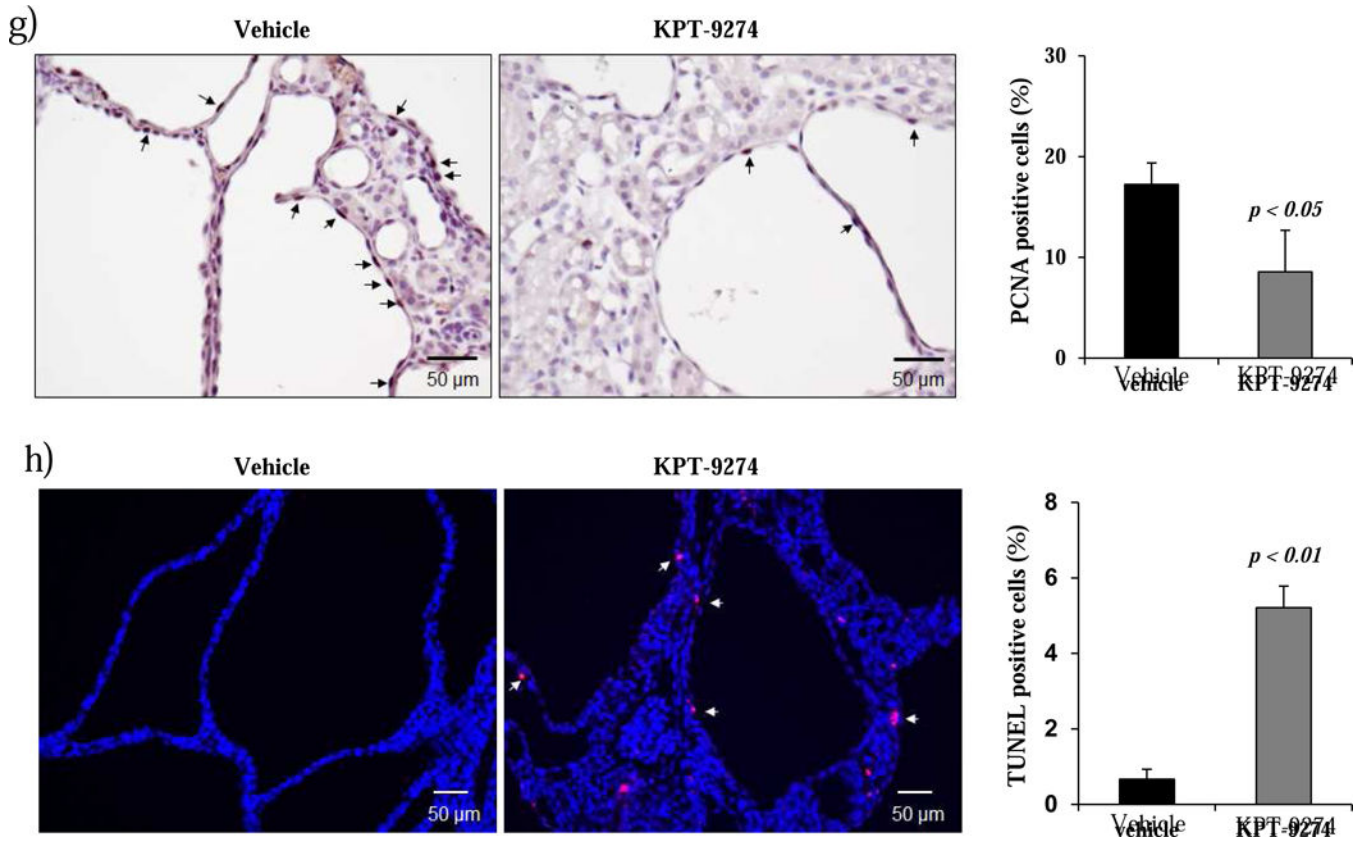

FIGURE 5.

KPT9274 treatment delays cyst growth *Pkd1*$^{flox/flox}$*:Pkhd1-Cre* mice.

(a) Kidneys from *Pkd1*$^{flox/flox}$*:Pkhd1-Cre* mouse kidneys and *Pkd1*$^{+/+}$*:Pkhd1-Cre* mice were treated for 15 days with KPT-9274 (IP; 60 mg/kg) and the kidneys were harvested 24 h after the last dose of KPT-9274, immunoblotted and probed with antibodies to total and phosphorylated β-catenin and β-actin as a loading control.

(b) Kidneys from *Pkd1*$^{+/+}$*:Pkhd1-Cre* mice were treated for 7 days with KPT-9274 (IP; 100 mg/kg) or vehicle. The mice were sacrificed 16 h after the last dose of KPT-9274, and lysates were subject to immunoblotting for total-PAK4, total-β-catenin, and β-actin as loading control. *p<0.05 compared to vehicle.

(c) H&E staining of *Pkd1*$^{flox/flox}$*:Pkhd1-Cre* mouse kidneys treated with vehicle or KPT-9274.

(d) Cystic index was quantified from sagittal sections of whole kidneys. Whole kidney images were acquired and total kidney area, cystic area and non-cystic area were measured by NIH Image J. Cystic index = (total cystic area ÷ total kidney area) × 100 and is expressed as a percentage. Data are means ± SD (n=8)

(e) Kidney weight/body weight (KW/BW) ratio was quantified as total kidney weight (n=2/mouse) divided by total body weight. Data are means ± SD (n=8)

(f) BUN was quantified by Quantichrom urea assay kit. Data are means ± SD (n=8)

(g) PCNA staining and (g) TUNEL assay of *Pkd1*$^{flox/flox}$*:Pkhd1-Cre* mouse kidneys treated with vehicle or KPT-9274. Data are means ± SD (n=8)

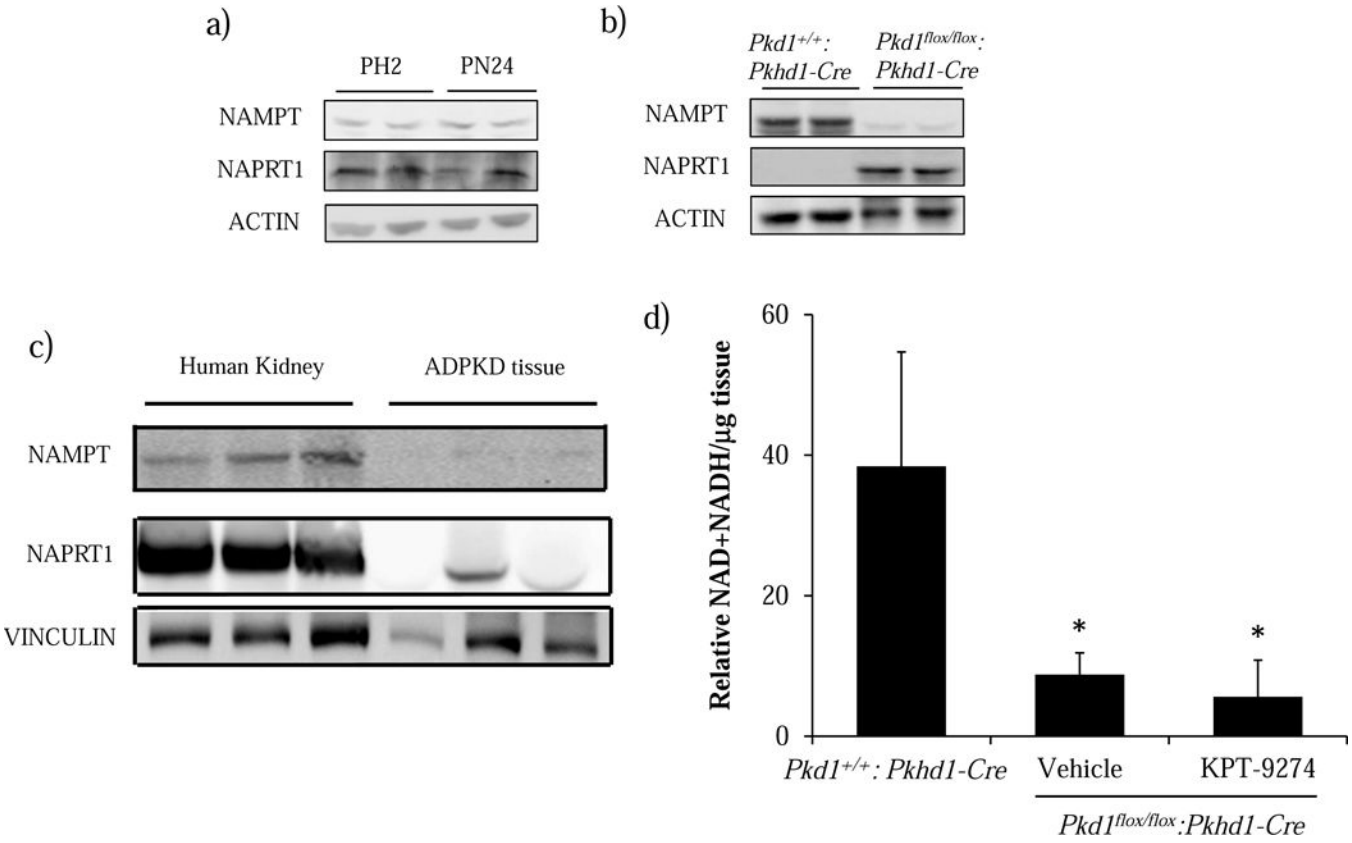

FIGURE 6.

The NAMPT inhibitory effect of KPT-9274 is likely not involved in cytogenesis inhibition. (a) Continuously growing PH2 and PN24 cells, (b) kidney tissues from untreated *Pkd1*$^{flox/flox}$*:Pkhd1-Cre* and *Pkd1*$^{+/+}$*:Pkhd1-Cre* mice, and (c) human ADPKD kidney and normal control tissue were immunoblotted for NAMPT and NAPRT1 and either β-actin or vinculin as loading controls.

(d) Tissues from *Pkd1*$^{+/+}$*:Pkhd1-Cre* mice, and *Pkd1*$^{flox/flox}$*:Pkhd1-Cre* mice, harvested 24 h after the last dose of either KPT-9274 or vehicle, were subjected to assays of total NAD +NADH as described in Materials and Methods. Data are means ± SD (n=3) from an average of 2 experiments. *P<0.05 compared to *Pkd1*$^{+/+}$*:Pkhd1-Cre* mice